Glycemic Control of People With Type 1 Diabetes Based on Probabilistic Constraints

Souransu Nandi, *Student Member, IEEE*, and Tarunraj Singh, *Senior Member, IEEE*

***Abstract*—The objective of the paper is to develop an open loop insulin infusion profile, which is capable of controlling the blood glucose level of people with Type 1 diabetes in the presence of broad uncertainties such as inter-patient variability and unknown meal quantity. For illustrative purposes, the Bergman model in conjunction with a gut-dynamics model is chosen to represent the human glucose-insulin dynamics. A recently developed sampling based uncertainty quantification approach is used to determine the statistics (mean and variance) of the evolving states in the model. These statistics are utilized to define chance constraints in an optimization framework. The solution obtained shows that under the assumptions made on the distribution of the model parameters, all possible glucose trajectories over time satisfy the desired glycemic control goals. The solution is also validated on the FDA approved Type 1 Diabetes Metabolic Simulator suggesting that the proposed algorithm is highly suitable for human subjects.**

***Index Terms*—Type 1 diabetes, chance constraints, uncertainty quantification, sequential cone programming.**

I. Introduction

PEOPLE suffering from Type 1 Diabetes lose their ability to synthesize natural insulin from their pancreas. Administration of exogenous insulin forms the only method of treatment today for their survival. This is done either manually with the help of subcutaneous injections of insulin before meals or by using an insulin pump. Calculation of the insulin dosages requires patients to be particularly cognizant of their own glucose levels, diet and daily activity levels. Even then, the risk of hyperglycemia and hypoglycemia is never absent. This puts severe limitations on the quality of life of the patient considering Type 1 diabetes is a chronic disease which requires daily monitoring over the patient's lifetime.

To alleviate the burden of self treatment and make the procedure safer, the biomedical engineering community has made significant progress towards building a device that can mimic the behaviour of a natural pancreas, called the *Artificial Pancreas* (AP) [1]. An AP comprises of a control algorithm which determines the required insulin to regulate blood glucose level variations caused by: meals, exercise, hormonal fluctuation, stress, etc. Specifically, the objective of the algorithm is to determine the insulin dosage needed to maintain the glucose level within normal limits over all time. This prescribed output of the algorithm is then fed to the insulin pump for infusion. The AP also integrates Continuous Glucose Monitoring (CGM) technology, which can serve as an input to the algorithm.

Several researchers have made contributions towards developing control algorithms for the AP over the past decade (See [2]–[4] and references therein). Lunze *et al.* [5] review the state of the art in controller design for people with type 1 diabetes. They tabulate a spectrum of control algorithms ranging from traditional PID controllers to adaptive MPC controllers. They conclude their paper by listing some of the outstanding problems that need to be resolved before an artificial pancreas can be widely deployed. In the development of most algorithms, the human glucose insulin dynamics are represented by a dynamic mathematical model. However, a major challenge in this framework remains accounting for the variability that exists in the true human glucose insulin dynamics between patients and even within a patient. The variability stems from the fact that the human body reacts differently depending on the time of day, the type and quantity of meals, current blood glucose levels and even levels of stress.

To account for this inter- and intra-patient variability, it is often assumed that the mathematical model is plagued with uncertain parameters. Principles of robust control theory, uncertainty quantification and stochastic systems can then be used to estimate parameter ranges as well as develop control algorithms for the stochastic mathematical model (For reference see [6]–[9]).

This paper presents a probabilistic problem formulation for the design of optimal controllers for people with Type 1 diabetes in the presence of model and meal uncertainties. The classical Bergman model is used to illustrate the proposed control formulation [10]. Since the traditional exponentially decaying models for glucose appearance in the Bergman model seem to depart from the glucose appearance rates from the FDA approved T1DMS simulator [11], a gut-dynamic model is included resulting in a sixth order model. A chance constraint, which only requires information of the mean and variance of the distribution of the blood-glucose is used to impose an acceptable risk level. We assume five uncertain parameters in the model, uncertainty in the meal size and uncertainty in the plasma glucose

Manuscript received January 31, 2018; revised July 12, 2018 and August 17, 2018; accepted August 30, 2018. Date of publication October 1, 2018; date of current version July 1, 2019. This work was supported by the National Science Foundation (NSF) under Awards No. CMMI-1537210. *(Corresponding author: Tarunraj Singh.)*

S. Nandi is with the Department of Mechanical Engineering, University at Buffalo, Buffalo, NY 14260 USA (e-mail: souransu@buffalo.edu).

T. Singh is with the Faculty of Department of Mechanical and Aerospace Engineering, University at Buffalo, Buffalo, NY 14260 USA (e-mail: tsingh@buffalo.edu).

Digital Object Identifier 10.1109/JBHI.2018.2869365

at the time of insulin bolusing. Since, we only require information about the mean and variance of the evolving blood-glucose, the recently developed Conjugate Unscented Transform (CUT) approach [12] is used to estimate the blood-glucose statistics. A sequential cone programming problem is then solved to determine the optimal insulin infusion profile to track an *ideal* glucose trajectory for the nominal meal.

This document is structured as follows. Section I introduces the problem statement and presents some background in the field. Section II delineates the system dynamics as well as articulates the environment used for the simulations. Section III provides a brief overview of the Conjugate Unscented Transform (CUT) and how it can be used to determine statistics of stochastic variables. This is followed by Section IV where the concept of chance constraints are introduced. Then, in Section V, the method to determine the statistics of blood glucose using CUT is explained. Section VI combines results from the previous two sections to present the implementation of the chance constraints on blood glucose distribution. The sequential cone programming algorithm is outlined in Section VII where the final results are presented. Section VIII then presents the validation of the resulting control profile on the T1DMS software. The paper concludes with closing remarks in Section IX.

II. Model and Simulation Environment

A. Dynamic Model

The mathematical model chosen in this work to represent the glucose-insulin dynamics in the human body is the Bergman's Minimal model [10]. It is defined by the dynamic equations:

$$\dot{G}(t) = -(X(t) + p_1)G(t) + p_1 G_b + R_{ag}(t)/V_g \tag{1}$$

$$\dot{X}(t) = -p_2 X(t) + p_3\,(I(t) - I_b) \tag{2}$$

$$\dot{I}(t) = \begin{cases} -p_4 I(t) + \gamma(G(t) - h)(t - t_m) & \text{for } t \geq t_m \text{ and} \\ & G(t) \geq h \\ -p_4 I(t) & \text{otherwise} \end{cases} \tag{3}$$

where p_1 $(\min^{-1})$, p_2 $(\min^{-1})$, p_3 $(\min^{-2} \cdot \text{L/mU})$, p_4 $(\min^{-1})$, γ $(\min^{-2} \cdot \text{mU} \cdot \text{dL/mg} \cdot L)$ and h (mg/dL) are model parameters. p_1 is used to characterize the effective glucose disappearance at basal insulin levels, while p_2 along with p_3 represents the capacity of insulin to increase glucose disappearance and hinder more glucose production. The states $G(t)$ (mg/dL), $X(t)$ $(\min^{-1})$ and $I(t)$ (mU/L) represent the blood (plasma) glucose concentration, (effective) insulin in the remote compartment and the plasma insulin concentration respectively. G_b and I_b represent certain basal values of the states $G(t)$ and $I(t)$. The term $\gamma(G(t) - h)(t - t_m)$ in equation (3) mimics the action of the human pancreas, t_m (which has been assumed to be 30 min for all simulations) is time of meal consumption and V_g (dL) is the distribution volume of glucose.

The additional term $R_{ag}(t)$ (mg) (also referred to as the Rate of appearance of glucose in plasma) is introduced in the model to replicate a meal intake disturbance. $R_{ag}(t)$ is evaluated using a human gut dynamics model adopted from the works of Dalla Man *et al.* in [13]. The model is given by the equations:

$$\dot{q}_{sto1}(t) = -k_{21} q_{sto1}(t) + D\delta(t - t_m) \tag{4}$$

$$\dot{q}_{sto2}(t) = -k_{empt} q_{sto2}(t) + k_{21} q_{sto1}(t) \tag{5}$$

$$\dot{q}_{gut}(t) = -k_{abs} q_{gut}(t) + k_{empt} q_{sto2}(t) \tag{6}$$

$$R_{ag}(t) = f k_{abs} q_{gut}(t) \tag{7}$$

$$q_{sto} = q_{sto1} + q_{sto2} \tag{8}$$

$$k_{empt}(q_{sto}) = k_{\min} + 0.5(k_{\max} - k_{\min})(\tanh\left[\alpha(q_{sto} - bD)\right] - \tanh[\beta(q_{sto} - cD)] + 2) \tag{9}$$

$$\alpha = \frac{5}{2D(1-b)} \tag{10}$$

$$\beta = \frac{5}{2Dc}; \tag{11}$$

where q_{sto1} (mg) and q_{sto2} (mg) are the amounts of glucose in solid and liquid phases respectively present in the stomach at any time. q_{gut} (mg) is the amount of glucose in the intestines, $\delta(.)$ is the Dirac delta function and D (mg) is the amount of glucose consumed during the meal in milligrams. k_{21} $(\min^{-1})$ is a constant which governs the rate of food movement from the first stomach state to the second. k_{empt} $(\min^{-1})$ represents the rate at which the food is drained from the second stomach state to the gut state. It is bounded by maximum and minimum values $k_{\max}$ and $k_{\min}$ respectively. k_{abs} $(\min^{-1})$ is the rate at which the carbohydrates are absorbed into the body from the gut. α and β are parameters which determine the transition of k_{empt} between its extremities. Finally, b, c and f are other dimensionless parameters of the model.

A schematic illustrative diagram of the Bergman model as well as the gut dynamics model can be found in [10] and [13] respectively. Details regarding the physiological parameters of these models can also be found in the said references.

One of the objectives of the control problem is to make the glucose concentration in people with Type 1 diabetes track the glucose concentration of a normal person over time after a meal. The variation of glucose concentration for a normal person is referred to as the target glucose trajectory. This target trajectory is generated by simulating the Bergman model using parameter values fit to a normal person and a meal size of 37.5 grams of carbohydrates. Since these parameters vary among people, a set of values are chosen, for illustrative purposes, from literature [14], [15]; where the Bergman model and the gut dynamics were actually fit to real data (taken from a normal subject(s)). These values are listed in Table I. The initial conditions for the trajectory was selected as:

$$G(0) = G_b;\;\; X(0) = 0;\; \text{and } I(0) = I_b.$$

It should be noted that during practical implementation, the parameters and initial conditions are not binding and can be altered depending on the target trajectory desired for a patient. It is entirely plausible that separate target trajectories may be required for patients with varying degrees of severity of the disease. In fact, the target trajectory need not be obtained from

TABLE I
PARAMETER VALUES FOR A NORMAL SUBJECT

Parameter	Value	Parameter	Value
p_1	0.03082	k_{max}	0.0558
p_2	0.02093	k_{min}	0.0080
p_3	1.062×10^{-5}	k_{abs}	0.057
p_4	0.30000	k_{21}	0.0558
γ	0.003349	b	0.82
h	89.5	c	0.00236
G_b	92	f	0.9
I_b	7.3	V_g	146.64

TABLE II
PARAMETER VALUES FOR A SUBJECT WITH TYPE 1 DIABETES

Parameter	Value	Parameter	Value
$p_1^{nominal}$	0.0287 ($\pm$0.0086)	$k_{max}^{nominal}$	0.0429 ($\pm$0.0129)
$p_2^{nominal}$	0.0283 ($\pm$0.0085)	$k_{min}^{nominal}$	0.0141 ($\pm$0.0042)
$p_3^{nominal}$	$5.035(\pm 1.51)E-5$	k_{abs}	0.2062
p_4	5/54	k_{21}	0.0558
γ	N/A	b	0.7612
h	N/A	c	0.1372
G_b	119.1858	f	0.9
I_b	15.3872	V_g	128.8237

a model simulation and could be prescribed by the respective physician. However, in this work as mentioned previously, for illustration, the target trajectory is obtained from a simulation.

The natural pancreas term ($\gamma(G(t)-h)(t-t_m)$) is removed from the model for people with Type 1 diabetes and is substituted by an artificial insulin input term $U'(t)$ similar to Lynch and Bequette in [16]. This alters equation (3) to

$$\dot{I}(t) = -p_4 I(t) + U'(t). \tag{12}$$

The diabetic model (comprised of equations (1), (2) and (12)) is now an unstable system in the absence of any insulin control causing the glucose concentration to grow unchecked (which is reasonable to assume: for a person with Type 1 diabetes with no insulin). To stabilize the glucose concentration in such patients, in reality, a basal insulin dosage is given. This concept can be modeled by assuming the control to be of the form

$$U'(t) = U(t) + p_4 I_b \tag{13}$$

where the term $p_4 I_b$ mimics the basal dosage. With this modification, the diabetic model can be summarized as:

$$\dot{G}(t) = -(X(t)+p_1)G(t) + p_1 G_b + R_{ag}(t)/V_g \tag{14}$$

$$\dot{X}(t) = -p_2 X(t) + p_3(I(t)-I_b) \tag{15}$$

$$\dot{I}(t) = -p_4(I(t)-I_b) + U(t). \tag{16}$$

Equations (14) through (16) now represent a stable system where the glucose concentration is driven to the desired basal level (G_b). The objective is to determine an insulin trajectory ($U(t)$) that can be administered intravenously (IV) to successfully track the target trajectory to accommodate consumption of meals.

B. Model Uncertainties

This subsection is used to outline the uncertainties that have been assumed in the mathematical model to account for patient variability. It also presents the values for the non-uncertain parameters.

In this work, $G(0)$, p_1, p_2, p_3, $k_{\max}$ and $k_{\min}$ are assumed to be uncertain. k_{21} is equal to $k_{\max}$ and is therefore also uncertain [13]. The non-uncertain Bergman parameter p_4 is taken from literature [16] where the value was identified by fitting the Bergman model to the outputs obtained from the Sorensen diabetic model. The other non-uncertain parameters for people with diabetes (k_{abs}, b, c, f, V_g G_b and I_b) were obtained from the FDA approved Type 1 Diabetes Metabolic Simulator (T1DMS) software (corresponding to an average adult). The parameters have been tabulated in Table II.

$G(0)$ is the glucose concentration in plasma when the simulation starts (i.e., at $t = 0$ min). Since, the glucose concentration at that instant is unlikely to be exactly the basal value (G_b), $G(0)$ is assumed to be uniformly distributed about G_b with a 30% variation on either side of it. Therefore, $G_0 \in U[83.43, 154.9415]$ is used to characterize the uniformly distributed uncertain initial value of glucose.

To account for inter-patient variability p_1, p_2, p_3, $k_{\min}$ and $k_{\max}$ are also assumed to have uniform distributions with a 30% variation about their nominal values. The nominal values (for people with Type 1 diabetes) are taken from literature [16] and T1DMS average adult data set (Table II). The variation ranges of the uncertain parameters are quoted in parenthesis along with their nominal values.

The final uncertainty has been assumed in the meal size consumed by a patient (i.e., the parameter D in equation (4)). According to the 2010 Dietary Guidelines [17] published by the U. S. Department of Agriculture, Health and Human Services, the daily carbohydrate (CHO) intake goal for all ages should be 130 gm. Depending on the individual and time of day, meal sizes can vary. Light and heavy meals vary in their CHO counts significantly. The values can vary between 15 gm for a snack to 60 gm for lunch if CHOs from all foods at a meal are added up. A breakdown of the CHO content of recommended foods for people with diabetes can be found in article [18] from the American Diabetes Association. Based on the daily total and mealtime CHO recommendations, D is conservatively assumed to have a uniform distribution given by $D \in U[15000, 60000]$ mg.

All the aforementioned uncertainties are time invariant and their impact on the evolution of the blood glucose is of interest in the analysis of any controller. Monte Carlo simulations can be used to estimate the evolution of the probability density function of the blood-glucose. However, it is well recognized that this is computationally expensive and will not be suitable for real-time estimation of the time evolution of the statistics of the blood-glucose. A technique such as polynomial chaos [19] presents a powerful approach for the estimation of the statistics, but also suffer from the curse of dimensionality as the number of uncertain variables increase. A powerful deterministic sampling based approach was proposed by Julier and Uhlman [20], called the Unscented Transform (UT). UT permits using $2p+1$ number of samples (sigma points) for p dimensional uncertain inputs to estimate the mean and covariance of the output. One

shortcoming of the UT is that as the number of uncertain variable grows, the weights assigned to the sigma points can become negative and the location of the sigma points can lie outside the support of the uncertain variable. For example, if a variable is uniformly distributed, the sigma points could potentially fall outside the support of the uncertain variable. This motivates the use of a more sophisticated method to calculate statistics of random variables. The next section outlines a recently developed sampling scheme that addresses the aforementioned issues.

III. Conjugate Unscented Transform

The Conjugate Unscented Transform (CUT) for multivariate uniform distributions introduced in [12] is a technique used to calculate statistics of uniform random variables which undergo nonlinear transformations. It belongs to a wide class of techniques commonly referred to as sigma-point based estimators. In these methods, a set of points (a.k.a. the sigma points) are selected from the uncertain space (whose statistics are known) such that the mean and the covariance of all the points match with the known statistics. Each of these points are then made to go through the non-linear transformation to yield another set of points in the transformed space. The statistics of the transformed space is now evaluated from the transformed points by weighing them appropriately.

The CUT defines a way to determine the position (x_i) and the associated weights (w_i) of these sigma points. If the non-linear transformation is defined as $y_i = f(x_i)$, then the statistics (mean and covariance) of the transformed space (y) is determined by

$$\overline{y} = \sum_{i=1}^{N} w_i y_i \text{ and} \tag{17}$$

$$P_y = \sum_{i=1}^{N} w_i (y_i - \overline{y})(y_i - \overline{y})^T \tag{18}$$

respectively where N is the total number of sigma points, $\overline{y}$ and P_y are the mean and the covariance of the transformed variable.

For the diabetes problem considered in this work, CUT is used to depict the variation in the glucose concentration due to the assumed uncertainties. The number of uncertainties is 7 (i.e., $\boldsymbol{x} = [p_1, p_2, p_3, G(0), D, k_{\max}, k_{\min}]^T$). It should be noted that since k_{21} is equal to $k_{\max}$, the dimensionality of the uncertainties remains seven. Since, the variable of interest is the glucose concentration, the output y is $G(t)$ and the non-linear function f is the numerical simulation of the diabetic model (equations (14) through (16)). After assuming that the uncertain variables are independent, $N = 686$ sigma points ($\boldsymbol{x}^{(i)}$) and weights ($w^{(i)}$) are generated using the CUT-4 algorithm [12]. For each of these sigma points, the diabetic model is simulated and the glucose trajectories over time are recorded. The statistics of the glucose concentration (at each time instant) is then evaluated by weighing all the trajectories appropriately (as presented in equations (17) and (18)). Fig. 1 shows a 3-sigma bounded variation of the glucose concentration, calculated from the 686 trajectories via CUT.

It is recommended that plasma glucose concentration never falls below a lower bound G_{lb} (hypoglycemia) at any time.

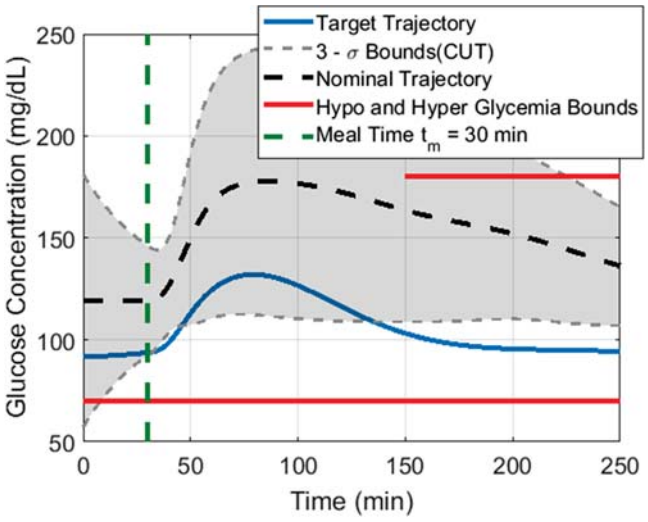

Fig. 1. Glucose variation with only basal Insulin infusion, i.e., $U(t) = 0$.

According to a joint consensus statement from the ADA and the Endocrine Society regarding hypoglycemia and diabetes [21], the threshold for hypoglycemia (G_{lb}) should be $70\frac{\text{mg}}{\text{dL}}$. In addition, after two hours (120 min) of a meal, it is recommended by the American Diabetes Association [22] that the plasma glucose concentration be below $180\ \frac{\text{mg}}{\text{dL}}$. These constraints have been shown (in red) in Fig. 1 as well. The objective now is to figure out a way to incorporate these constraints into the control problem. One way to do it would be to pose hard inequality constraints on the blood glucose at the necessary time instants. However, a downside to this approach is that the hypoglycemic as well as the hyperglycemic constraints are treated with equal severity where in reality it is accepted that the hyperglycemic constraint is a comparatively softer constraint (as compared to the hypoglycemic one) in the short term. Moreover, assuming hard constraints may also fail to give a feasible control solution where significant variability in glucose trajectories have been assumed. As a result, these two issues motivate a probabilistic approach towards the glycemic constraints. The next section introduces the concept of chance constraints which is used later to impose probabilistic constraints on blood glucose uncertainty.

IV. Chance Constraints

Calafiore and El Ghaoui in [23] provide an approach to rewrite linear probabilistic inequalities as deterministic inequalities. In their work, they prove that if a and b are random variables with known means and variances, then the constraint:

$$\text{Prob}\left\{a^T x + b \leq 0\right\} \geq 1 - \epsilon \tag{19}$$

is conservatively approximated by the convex constraint

$$\sqrt{\frac{1-\epsilon}{\epsilon}}\left\{\text{var}\left[a^T x + b\right]\right\}^{1/2} + E\left[a^T x + b\right] \leq 0 \tag{20}$$

where ϵ ($\in (0,1)$) represents the risk level i.e., the probability with which the constraint is permitted to be violated. It should be noted that the constraint is conservative since it subsumes all distributions with the same mean and variance. Therefore,

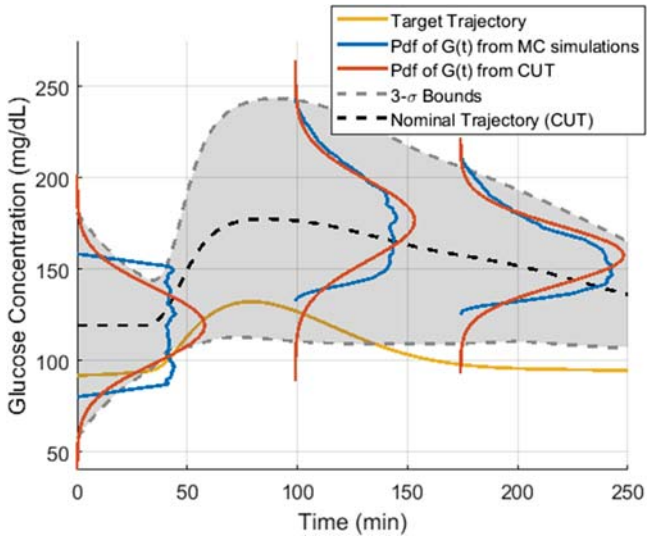

Fig. 2. Pdfs obtained from CUT and MC sampling at times: $t = 0$, 99 and 174 min. (Pdfs have been scaled for illustration).

if only the first two moments of the random variables (a, b) are known, equation (20) allows one to enforce equation (19) no matter what the true distribution of (a, b) is. However, since this constraint is robust to all distributions, it yields conservative solutions.

One alternative would be to assume a Gaussian distribution as the probability distribution function (pdf) of $G(t)$ and enforce a chance constraint specific to a Gaussian distribution. However, from Fig. 2 which illustrate the pdf of $G(t)$ one can conclude that it is non-Gaussian at all times.

In Fig. 2, Gaussian pdfs are generated using the mean and variance obtained from CUT at 3 distinct time instants (shown in red). These pdfs are then compared to the pdfs generated from 10000 MC sample trajectories (shown in blue). It is evident that although the two sets of pdfs have the same first two moments, they are all different. Hence, the robust chance constraint (equation (20)) is chosen for implementation.

The idea here is to first: use CUT to obtain accurate measures of the mean and the variance of plasma glucose $(G(t))$ over time and then: use these measures to enforce hypoglycemic or hyperglycemic chance constraints.

V. Computation of Mean and Variance

The formulation of the chance constraints is designed only for linear constraints (Equation (19)). Such a formulation would need the mean of $G(t)$ to be a linear function of $G(0)$ and $U(t)$ as well as the variance of $G(t)$ to be a quadratic function of $G(0)$ and $U(t)$. This is not the case here as can be seen from the model equations. Therefore, the first objective of this section is to present a linear approximation for $G(t)$ which can cater to the chance constraint needs. The second objective is to derive a way in which the statistics of blood glucose can be determined after the control input has been slightly perturbed.

To deal with the issue of non-linearity, the non linear model is linearized about the trajectories generated from the N sigma points (also called the nominal trajectories). The mean and the variance of $G(t)$ are then calculated from these linearized models by appropriately weighing them. This entire process is elaborated in this section.

A. Linearization

Let the non-linear diabetes model be described by the equation

$$\dot{\boldsymbol{z}} = \boldsymbol{f}(\boldsymbol{z}, U) \tag{21}$$

where $\boldsymbol{z} = [G, X, I, q_{sto1}, q_{sto2}, q_{gut}]^T$. This system is linearized about the N nominal trajectories $\overline{\boldsymbol{z}}^{(i)}$. $\overline{\boldsymbol{z}}^{(i)}$ are generated from N sigma points using $\dot{\overline{\boldsymbol{z}}}^{(i)} = \boldsymbol{f}(\overline{\boldsymbol{z}}^{(i)}, \overline{U})$, where $\overline{U}$ (also referred to as the nominal input) is an initial guess of the control input U. The error dynamics of the linearized systems is given by

$$\Delta\dot{\boldsymbol{z}}^{(i)} = \left.\frac{\partial \boldsymbol{f}}{\partial \boldsymbol{z}}\right|_{\boldsymbol{z}=\overline{\boldsymbol{z}}^{(i)}, U=\overline{U}} \Delta\boldsymbol{z}^{(i)} + \left.\frac{\partial \boldsymbol{f}}{\partial U}\right|_{\boldsymbol{z}=\overline{\boldsymbol{z}}^{(i)}, U=\overline{U}} \Delta U \tag{22}$$

where (i) represents the system corresponding to the ith sigma point and varies from 1 to N. This linear system is now discretized so that linear algebraic chance constraints on the blood glucose can be exercised.

B. Discretization

The discretized version of equation (22) assuming a Zero Order Hold setting can be written as

$$\Delta\boldsymbol{z}^{(i)}(k+1) = A_k^{(i)}\Delta\boldsymbol{z}^{(i)}(k) + B_k^{(i)}\Delta U(k) \tag{23}$$

where k is the kth time step, $A_k^{(i)}$ and $B_k^{(i)}$ are state dependent discretized system matrices for the ith sigma point trajectory. Equation (23) can be simplified to

$$\Delta\boldsymbol{z}^{(i)}(k+1) = \left(\prod_{j=0}^{k} A_j^{(i)}\right)\Delta\boldsymbol{z}^{(i)}(0) + B_k^{(i)}\Delta U(k) + \sum_{j=0}^{k-1}\left(\prod_{m=j+1}^{k} A_m^{(i)}\right) B_j^{(i)}\Delta U(j) \tag{24}$$

where $\Delta\boldsymbol{z}^{(i)}(0)$ represents the initial perturbation state of each trajectory and is equal to 0.

For the entire work, the simulation time has been assumed to be $T_f = 250$ min and the sampling time to be $T_s = 1$ min. This makes k vary between 0 and 249. Correspondingly, the number of inputs is 250, i.e., $U(0)$ through $U(249)$. If the entire control profile is defined by the vector $\boldsymbol{U} = [U(0), U(1), \ldots, U(249)]^T$, the entire blood glucose profile by $\boldsymbol{G} = [G(1), G(2), \ldots, G(250)]^T$), the perturbation dynamics can be given by the equation

$$\Delta\boldsymbol{G}^{(i)} = M^{(i)}\Delta\boldsymbol{U} \tag{25}$$

where $M^{(i)} =$

$$\begin{bmatrix} C_{glu}B_0^{(i)} & \cdots & & \\ C_{glu}A_1^{(i)}B_0^{(i)} & C_{glu}B_1^{(i)} & & \\ \vdots & \vdots & \ddots & \\ C_{glu}\left(\prod_{j=1}^{k} A_j^{(i)}\right)B_0^{(i)} & \cdots & \cdots & C_{glu}B_{249}^{(i)} \end{bmatrix} \tag{26}$$

and $C_{glu} = [1, 0, 0, 0, 0, 0]$. Thus, equation (25) allows us to write the blood glucose perturbation along each sigma point trajectory as a linear function of the input perturbation, accomplishing the first objective of the section.

C_{glu} can also be used to write the nominal blood glucose trajectories as

$$\overline{\boldsymbol{G}}^{(i)} = C_{glu}\boldsymbol{z}^{(i)}. \tag{27}$$

Therefore, the blood glucose profile $\boldsymbol{G}$ due to a $\Delta\boldsymbol{U}$ change in the control input profile $\overline{\boldsymbol{U}}$ can be finally written as

$$\boldsymbol{G} = \overline{\boldsymbol{G}} + \Delta\boldsymbol{G} \tag{28}$$

where $\overline{\boldsymbol{G}} = \sum_{i=1}^{N} w_i \overline{G}^{(i)}$, is the stochastic nominal blood glucose trajectory due to the control input $\overline{\boldsymbol{U}}$ and $\Delta\boldsymbol{G}$ is the stochastic perturbation about $\overline{\boldsymbol{G}}$ due to a perturbation in the control input $\Delta\boldsymbol{U}$. The statistics of $\boldsymbol{G}$ can now be easily calculated using relations similar to (17) and (18) since we have $\overline{\boldsymbol{G}}$ as well as sigma-point realizations of $\Delta\boldsymbol{G}$. This completes the second objective.

However, the statistics of most interest is the mean and the variance of $\boldsymbol{G}$ because the mean and the variance are the only two moments necessary for the robust chance constraints. The next section details the development of the chance constraints using the said two moments.

VI. Chance Constraints on Glucose

As expressed previously, this work seeks to implement chance constraints on the hypoglycemic and hyperglycemic blood glucose concentration levels. It is desired that the hypoglycemic constraint is always satisfied, i.e., $G(k) \geq G_{lb}$ for all k. It is also desired that the hyperglycemic constraint is satisfied after two hours of the meal, i.e., $G(k) \leq G_{ub}$ for $k > 150$ since meal time is $t_m = 30$ min. In this section, the derivation of only the hypoglycemic chance constraint at a particular time instant j is shown, as the other constraints are almost identical. The objective of this section is to derive a convex inequality as a function of $\Delta\boldsymbol{U}$ to represent the chance constraints.

The blood glucose concentration at the jth minute is given by the jth row of equation (28) and is summarized as $G(j) = \overline{G}(j) + \Delta G(j)$. The goal is to effectively implement the following probabilistic constraint

$$\text{Prob}\left\{-G(j) + G_{lb} \leq 0\right\} \geq 1 - \epsilon_1 \text{ for } j = 1, \ldots, 250. \tag{29}$$

Ideally, ϵ_1 should be nearly 0 since we want the hypoglycemic constraint to be satisfied with near probability 1. However, since the chance constraints are conservative to begin with, a 20% violation is allowed, i.e., $\epsilon_1 = 0.2$. Equation (29) is equivalent to the constraint

$$\sqrt{\frac{1-\epsilon_1}{\epsilon_1}}\left\{\text{var}\left[-G(j) + G_{lb}\right]\right\}^{1/2} + E\left[-G(j) + G_{lb}\right] \leq 0 \tag{30}$$

similar to equation (20). Now,

$$\begin{aligned} E[-G(j) + G_{lb}] &= -E[\overline{G}(j) + \Delta G(j)] + G_{lb} \\ &= -\underbrace{\sum_{i=1}^{N} w^{(i)}\overline{G}^{(i)}(j)}_{E\left[\overline{G}(j)\right]} - \underbrace{\sum_{i=1}^{N} w^{(i)} M_j^{(i)}\Delta\boldsymbol{U}}_{E\left[\Delta G(j)\right]} + G_{lb} \end{aligned} \tag{31}$$

where $\overline{G}^{(i)}(j)$ is the jth element of $\overline{\boldsymbol{G}}^{(i)}$ and $M_j^{(i)}$ is the jth row of $M^{(i)}$. Moreover,

$$\text{var}\left[-G(j) + G_{lb}\right] = \text{var}[-G(j)] = \text{var}\left[\overline{G}(j) + \Delta G(j)\right] \tag{32}$$

since G_{lb} is a number and not a random variable. Continuing with the development, we get

$$\begin{aligned} \text{var}\left[\overline{G}(j) + \Delta G(j)\right] = \text{var}\left[\overline{G}(j)\right] + \text{var}[\Delta G(j)] \\ + 2\text{cov}[\overline{G}(j), \Delta G(j)]. \end{aligned} \tag{33}$$

The variances can be found using the following relations

$$\text{var}[\overline{G}(j)] = \underbrace{\sum_{i=1}^{N} w^{(i)}\left(\overline{G}^{(i)}(j) - E\left[\overline{G}(j)\right]\right)^2}_{C} \text{ and} \tag{34}$$

$$\text{var}[\Delta G(j)] = \sum_{i=1}^{N} w^{(i)}\left(\Delta G^{(i)}(j) - E\left[\Delta G(j)\right]\right)^2. \tag{35}$$

Equation (35) can be simplified in terms of $\Delta\boldsymbol{U}$ as

$$\text{var}[\Delta G(j)] = \Delta\boldsymbol{U}^T \underbrace{\left(\sum_{i=1}^{N}(M_j^{(i)} - M_j)w^{(i)}(M_j^{(i)} - M_j)^T\right)}_{A}\Delta\boldsymbol{U}. \tag{36}$$

where $M_j = \sum_{i=1}^{N} w^{(i)} M_j^{(i)}$. The covariance term in equation (33) is found using

$$\text{cov}\left[\overline{G}(j), \Delta G(j)\right] = \sum_{i=1}^{N} w^{(i)}\left(\overline{G}^{(i)}(j) - E[\overline{G}(j)]\right)\left(\Delta G^{(i)}(j) - E[\Delta G(j)]\right). \tag{37}$$

Once again, equation (37) can be simplified in terms of $\Delta\boldsymbol{U}$ as

$$\text{cov}\left[\overline{G}(j), \Delta G(j)\right] = \underbrace{\left(\sum_{i=1}^{N} w^{(i)}\left(\overline{G}^{(i)}(j) - E\left[\overline{G}(j)\right]\right)\left(M_j^{(i)} - M_j\right)\right)}_{B}\Delta\boldsymbol{U}. \tag{38}$$

Therefore, the variance term in equation (30) can be written as a quadratic function of the $\Delta \boldsymbol{U}$ vector as

$$\text{var}\left[-G(j)+G_{lb}\right] = \Delta \boldsymbol{U}^T A \Delta \boldsymbol{U} + 2B\Delta \boldsymbol{U} + C \tag{39}$$

where A, B and C are defined through equations (36), (38) and (34) respectively. Since $\text{var}[-G(j)+G_{lb}] \geq 0$, a factorization can be found of the form

$$\text{var}\left[-G(j)+G_{lb}\right] = \left(P\Delta \boldsymbol{U}+Q\right)^T \left(P\Delta \boldsymbol{U}+Q\right) \tag{40}$$

in which case we get

$$\text{var}\left[-G(j)+G_{lb}\right]^{1/2} = ||P\Delta \boldsymbol{U}+Q||_2. \tag{41}$$

On substituting equations (41) and (31) in (30), the chance constraint finally reduces down to the cone constraint

$$\underbrace{\sqrt{\frac{1-\epsilon_1}{\epsilon_1}}||P\Delta \boldsymbol{U}+Q||_2 - E\left[\overline{G}(j)\right] - E[\Delta G(j)] + G_{lb}}_{HypoCon(j)} \leq 0. \tag{42}$$

Equation (42) represents the hypoglycemic glucose chance constraint for the jth time instant or minute. By considering varying values of j, the hypoglycemic constraint can be imposed for every minute. A similar inequality can also be derived for the hyperglycemic constraint

$$\underbrace{\sqrt{\frac{1-\epsilon_2}{\epsilon_2}}||P\Delta \boldsymbol{U}+Q||_2 + E\left[\overline{G}(j)\right] + E[\Delta G(j)] - G_{ub}}_{HyperCon(j)} \leq 0. \tag{43}$$

in which case j would vary from 150 to 250. ϵ_2 is used to denote the risk level for the hyperglycemic constraint and since it is a much softer constraint, the value was fixed to be 0.3, i.e., allowing a 30% violation.

Now that all the components necessary to solve the optimal control problem have been defined, the next section focuses on the sequential cone programming algorithm (which uses results from all the previous sections) to finally solve it.

VII. Sequential Cone Programming

This section presents the iterative sequential algorithm that can be used to determine a solution to the optimal control problem.

The algorithm starts with an initial guess of the entire IV insulin control profile. This profile is also termed as the nominal control trajectory and is represented by $\overline{\boldsymbol{U}} = [\overline{U}(0), \overline{U}(1), \ldots, \overline{U}(249)]^T$. In the problem it is assumed that the control $\overline{\boldsymbol{U}}$ results in the stochastic state $\overline{\boldsymbol{G}}$ and the control $\boldsymbol{U} = \overline{\boldsymbol{U}} + \Delta \boldsymbol{U}$ results in the stochastic state $\boldsymbol{G} = \overline{\boldsymbol{G}} + \Delta \boldsymbol{G}$.

Using $\overline{\boldsymbol{U}}$ as the control input trajectory, N nominal state trajectories $\overline{\boldsymbol{z}}^{(i)}$ are determined based on the N sigma points. The sigma point trajectories now allow the determination of the mean and the variance of $\overline{\boldsymbol{G}}$ as weighted sums of the nominal glucose trajectories ($\overline{\boldsymbol{G}}^{(i)}$).

This step is followed by linearizing the state space model about those N nominal state trajectories to obtain N time-varying continuous linear systems. The N time-varying continuous linear systems are then discretized to obtain N time-varying discrete linear systems with system matrices $A_k^{(i)}$ and $B_k^{(i)}$ (as explained in Section V-A and V-B).

These N sets of system matrices are then used to construct N special matrices ($M^{(i)}$), which map the control perturbation profile ($\Delta \boldsymbol{U}$) to the glucose perturbations ($\Delta \boldsymbol{G}^{(i)}$) about the N nominal glucose trajectories ($\overline{\boldsymbol{G}}^{(i)}$). This allows the determination of the mean and the variance of $\Delta \boldsymbol{G}$ as a linear and a quadratic function of $\Delta \boldsymbol{U}$ respectively. At this point in the development, the following optimization problem is solved:

$$\begin{aligned}
\text{minimize}_{\Delta \boldsymbol{U}} \quad & ||E[\boldsymbol{G}] - \boldsymbol{G}_{target}||_2 \\
\text{subject to} \quad & HypoCon(j) \leqslant 0 \qquad \text{for } j = 1, \ldots, 250 \\
& HyperCon(j) \leqslant 0 \qquad \text{for } j = 150, \ldots, 250 \\
& \boldsymbol{U} \geqslant 0.
\end{aligned}$$

The cost function of the problem is designed to minimize the error norm between the expected value of the glucose trajectory ($E[\boldsymbol{G}]$) and the target glucose trajectory ($\boldsymbol{G}_{target}$) shown in blue in Fig. 1 so that the control solution drives the mean glucose of the person with Type 1 diabetes towards a glucose profile seen in a normal individual. The first two constraints refer to the hypoglycemic and the hyperglycemic chance constraints derived in the previous section (summarized by the inequalities (42) and (43)). The final constraint is to enforce the fact that insulin can only be added to the bloodstream (and not removed).

The optimization problem is convex since the cost is a 2-norm error function (where the error function is linearly dependent on the optimization variable $\Delta \boldsymbol{U}$), the chance constraints are cone constraints and the final constraint is a linear inequality. There are many efficient convex solvers available to solve such problems. For this work however, the CVX MATLAB toolbox [24] was used. Once the solution $\Delta \boldsymbol{U}^*$ is obtained, the control input solution is updated using the relation: $\boldsymbol{U}^{*(1)} = \overline{\boldsymbol{U}} + \Delta \boldsymbol{U}^*$.

This step concludes the first iteration with $\boldsymbol{U}^{*(1)}$ representing the control solution determined from the iteration. Since the solution at the end of iteration 1 is obtained as a perturbation about an initial guess nominal control trajectory $\overline{\boldsymbol{U}}$, it depends on the choice of $\overline{\boldsymbol{U}}$. To converge to at least a locally minimal control solution, the entire process is made iterative where the nominal trajectory $\overline{\boldsymbol{U}}$ for the second iteration is made equal to the control solution from the previous iteration, i.e., $\boldsymbol{U}^{*(1)}$. Therefore, we get $\overline{\boldsymbol{U}}|_{iter+1} = \boldsymbol{U}^{*(iter)}$ where $iter$ represents the iteration number in the algorithm. As the entire control problem is resolved by solving convex cone optimizations sequentially at each iteration, the phrase Sequential Cone Programming (SCP) is used to justify the process.

Fig. 1 shows the variation of glucose (with the mean $\boldsymbol{G}$ in black dashed line) when no insulin control is present. We can see that a large fraction of the grey area (which shows a $3-\sigma$ glucose variability bound) violates the hyperglycemic glucose constraint beyond the 150 min mark, thus motivating the need for an insulin control.

Results from the SCP are now presented. The SCP algorithm is started with an initial nominal guess for the control. The nominal guess is chosen based on the pre-meal bolus principle

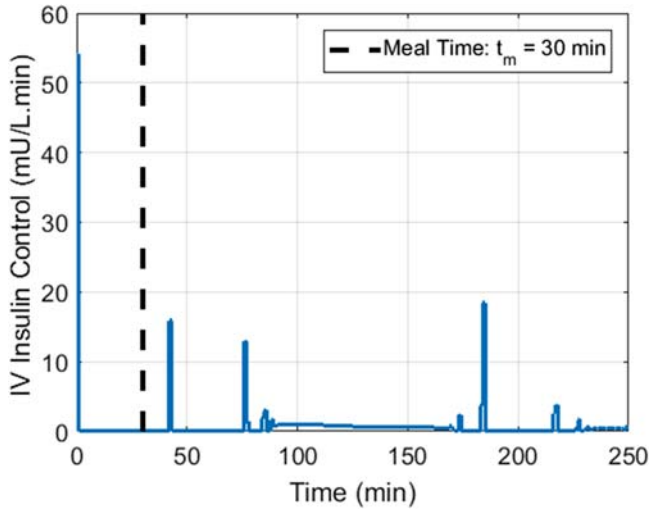

Fig. 3. Control solution $\boldsymbol{U}$ obtained after 9 iterations of the SCP.

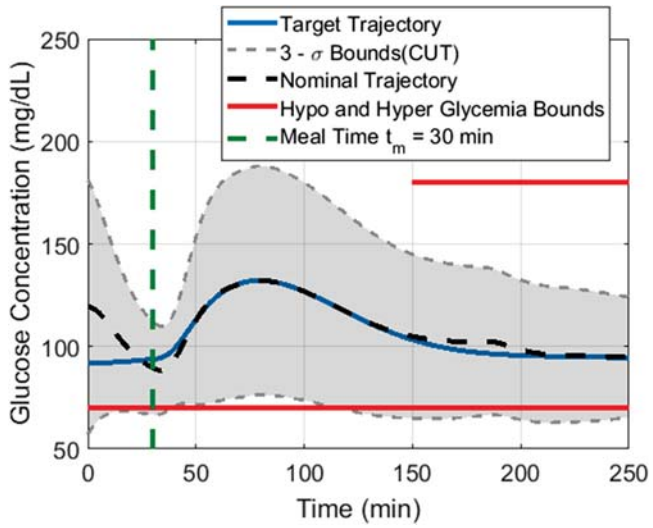

Fig. 4. Glucose variation $\boldsymbol{G}$ obtained after 9 iterations of the SCP.

where an insulin bolus is given prior to the consumption of every meal [25]. Therefore, the initial control guess is assumed to be $\overline{\boldsymbol{U}} = [40, 0, \ldots, 0]^T$.

It should be pointed out that the optimization assumes a linear approximation of the true non-linear model. Therefore finding a control solution for the linearized model which satisfies all the constraints does not imply that the same control on the true system would also satisfy those constraints. Hence, the SCP algorithm is terminated only if it is observed that the control solution is able to satisfy all the constraints even for the true non-linear system. In the illustrated case, the true glucose variation satisfied the desired constraints at the end of the 9th iteration. The control solution obtained at the end of the 9th iteration is shown in Fig. 3. Note that $t = 0$ corresponds to the time when the insulin infusion starts. The associated glucose variation (derived from the CUT algorithm) is shown in Fig. 4. In this figure we see that the glucose variation never violates the hyperglycemic limits. However, we do observe a consistent fraction of the variation to be violating the hypoglycemic bounds. This is because an allowance of 20% (i.e., $\epsilon_1 = 0.2$) was made and the SCP algorithm obtained a solution within those realms. Since perfect tracking of a normal person's glycemic behaviour is impossible, it is also seen that the nominal trajectory tracks the blue target trajectory as best it can (since the error between them was minimized).

It should also be mentioned that although the optimization problem being solved is a convex one, the final solution obtained need not be globally optimal. This is because the optimization problem tries to determine a perturbation profile about a pre-established control trajectory and not estimate the entire control input. Therefore, the optimization problem posed in this section only provides the best perturbation profile. Repeatedly solving this optimization problem (by updating the nominal control input) however, allows us to converge to a reasonable solution. It must also be mentioned that for an assumed $\overline{\boldsymbol{U}}$, a solution might not be feasible. This does not mean that a control input solution does not exist, but it just motivates the algorithm to select a better $\overline{\boldsymbol{U}}$.

VIII. Validation of Control Solution

The solution shown in Fig. 3 is specific to the target trajectory shown in Fig. 4. It should be noted that a different target trajectory would yield a different solution.

In order to check whether the solution control profile $\boldsymbol{U}^*$ is reasonable, it is tested on the FDA approved Type 1 Diabetes Simulator software [11] developed by the Epsilon Group. T1DMS was chosen because it is a well established simulator software for validation and has been extensively used by the diabetes research community ([26], [27]).

The solution is applied to 10 *in silico* adult subjects (similar to article [27]) and their glucose trajectories over time are monitored. The resulting trajectories have been shown in Fig. 5. Figs. 5(a), 5(b) and 5(c) correspond to simulations with distinct meals comprising 25 gm, 37.5 gm and 50 gm CHOs respectively. Although the control was obtained for up to 250 min mark, the simulations were executed up to 800 min to test the effects on the longer term. The insulin input $U(t)$ was zero between the time $t = 250$ and $t = 800$ which corresponds to a constant basal insulin infusion.

It can be seen that the glucose trajectories of the 10 adults are always within the allowed percentages of constraint violation after a meal. For the 25 gm meal case, at any instant in time, not more than 2 out of 10 (20%) cases ever violate the hypoglycemia bounds which is exactly the permitted percentage violations allowed during the determination of the control profile. Moreover, the authors would also like to say that, only one of the trajectories out of the two go severely low and violate the new definitions of clinical hypoglycemia which is defined by glucose levels $\leq$54 mg/dL (see reference [28]). Similarly, for the 37.5 gm meal case, we observe only a single hypoglycemia constraint violation. Finally, for the 50 gm meal case, only a single hypoglycemia and for the first time a couple of hyperglycemia violation is observed at an instant in time.

Therefore, the obtained insulin control profile solution is successful at maintaining the glucose levels of a variety of adult

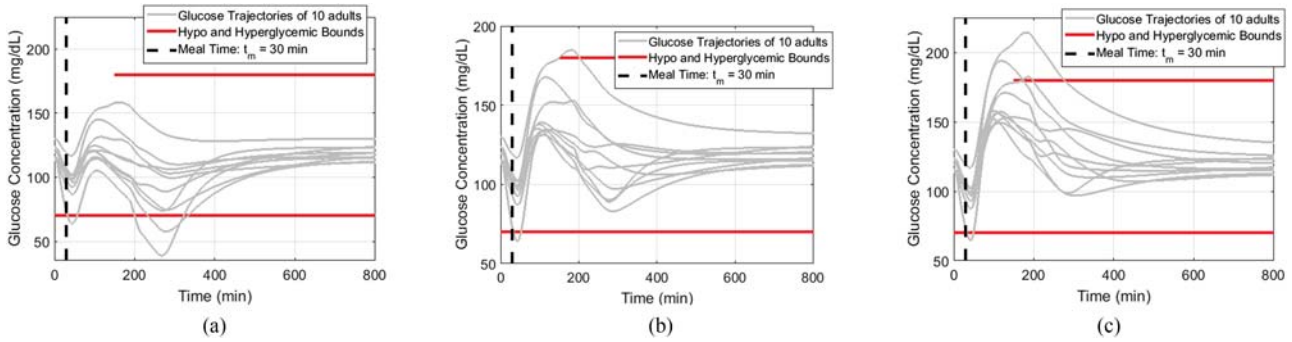

Fig. 5. Results from T1DMS software simulations for 3 distinct meal scenarios (SCP based design).

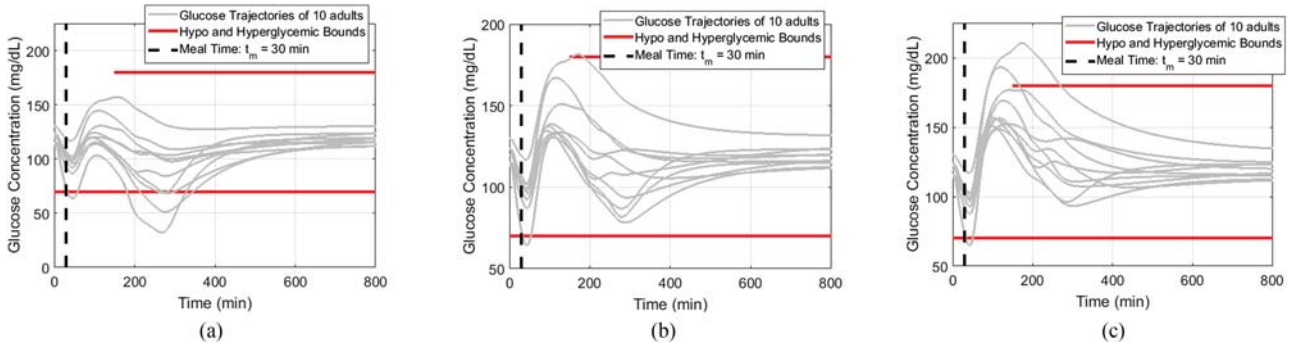

Fig. 6. Results from T1DMS software simulations for 3 distinct meal scenarios (Nominal model based design).

patients within the stipulated limits and within the risk limit prescribed in the design.

The open loop solution obtained in this paper can be motivated to be used in a Model Predictive Control (MPC) framework. The optimization problem can be solved to obtain an initial control profile. This solution can be implemented for a first few minutes (say for example 10 min) until a glucose observation is made. The optimization problem can be re-solved again after incorporating the observed glucose observation and the new solution could be again implemented over the next 10 min window. This framework of MPC could be exercised by re-solving the algorithm every 10 min to deal with the variability of the human glucose-insulin physiological dynamics and allow a form of feedback correction into the algorithm.

Under assumptions of model uncertainties, nominal models have been used to implement MPC in the literature before. Bemporad and Morari in [29] make an appropriate distinction in the robust analysis of MPC algorithms where they talk about two distinct methods of MPC design. One, which involves an MPC design on the nominal model without taking into consideration uncertainty and two, where the design process itself considers model uncertainties.

Hence, in this paper, for purposes of comparison, a control solution is derived by using a nominal model (i.e., using parameters from Table II) to track the target trajectory. Performance of this nominal control solution is then tested on the T1DMS for meal sizes identical to the SCP solution and presented in Figs. 6(a), 6(b), and 6(c). It should be pointed out that these two algorithms: the nominal one and the SCP based one correspond to the distinct design strategies alluded to in [29].

From Fig. 6 we see that although for meal sizes 37.5 gm and 50 gm the nominal model design does well, it does very poorly for the 25 gm meal size. Four trajectories are seen to be violating the hypoglycemic bounds with two of them going dangerously low (i.e., <54 mg/dL). In comparison, the SCP based design only allows two trajectories to violate the hypoglycemic bound and performs reasonably well for other meals. Moreover, for the SCP based design, the allowance of hypoglycemic violation (which was set at $\epsilon_1 = 0.2$) can be changed to suit the user. The value can be reduced further if stricter restrictions are needed for hypoglycemia. This flexibility in the design process is not available in a nominal model based design: hence providing one more advantage of the SCP over the nominal model design.

To study the effect of ϵ_1 and ϵ_2, the optimization problem was re-solved for some other combination of $\boldsymbol{\epsilon} = [\epsilon_1, \epsilon_2]^T$ values and the corresponding results have been presented in Fig. 7. The percentage of time spent *inside* the acceptable glycemic region has often been considered a metric of quality for any control strategy under scrutiny [30]. In this work, however, a complement of that metric which is defined as the percentage of time spent *outside* the acceptable glycemic region is considered to evaluate the quality of the derived control. Moreover, this metric is derived for each scenario (i.e., ϵ_1 and ϵ_2 combination) and comparisons are made to show the influence of $\boldsymbol{\epsilon}$. Ideally, lower the time spent outside the euglycemic region, better is the control algorithm.

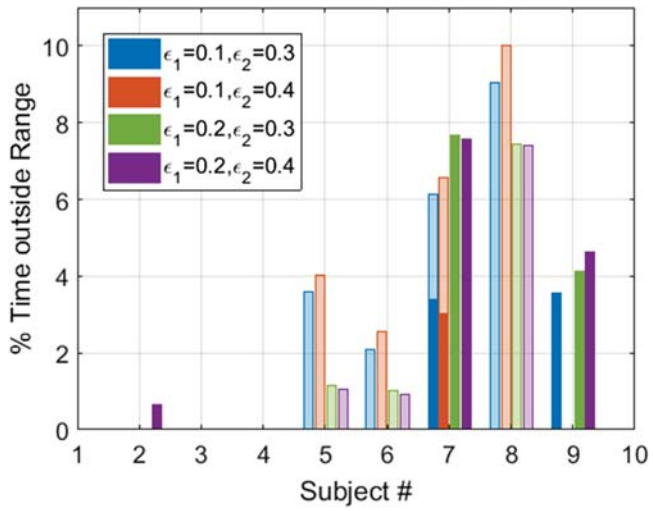

Fig. 7. Percentage of time spent outside euglycemic region for each ϵ case.

For each of the ϵ cases (the ϵ values for each case is quoted in Fig. 7), a new control solution was derived. This control was then used to simulate the glucose dynamics of 10 adult subjects in T1DMS for meal sizes of 25, 37.5 and 50 gms. This means, we obtained 3 glucose trajectories for each subject for each ϵ case (i.e., a total of 120 trajectories from 4 control solutions; 30 of which are shown in Fig. 5 while the rest have been presented in *Supplementary Materials*). The total time spent outside the euglycemic region for all the meal sizes were then added and evaluated as a percentage of the total time of simulation for each subject and each ϵ (which means we get 40 values for time of hypo- and hyper- glycemic violations since we have 4 ϵ cases and 10 subjects).

Fig. 7 is used to present this data in the form of a bar graph. Four colors are used to distinguish the four cases studied and color intensities are used to distinguish between the hypo (darker intensity)- and hyperglycemic (lighter intensity) excursions. The bars of different intensities have been stacked on top of each other to represent the total percentage of time spent outside the euglycemic region. We see that subjects 1-4 and 10 hardly show any transgressions. However, valuable insight can be drawn from subjects 5-9. The first thing to notice is that the first two bars and the last two bars of each subject are very similar. This means that the effect of ϵ_2 is not significant. This observation can be attributed to the fact that the hyperglycemic constraints during the design process is not active. As can be seen in Fig. 4, the hyperglycemic bounds are never violated for the Bergman + Gut dynamics model. Hence, on relaxing the risk of hyperglycemic violation, significant changes to the control solution does not occur and therefore we obtain similar violations. The second significant thing to notice is that the last two lightly colored bars are consistently lower than the first two lightly colored bars for any subject. This means that ϵ_1 does have an effect on the control solutions as expected. As the allowance of hypoglycemic bound violation is increased (from 0.1 to 0.2), the glucose trajectories tend to get pushed down leading to fewer hyperglycemic violations. The other obvious result as seen in subjects 7 and 9 is that, with an increase in ϵ_1, the magnitude of the solid bars have increased which is again consistent with our design process. It says that as more violations of hypoglycemia are permitted during the design process, more hypoglycemic violations take place on the actual in-silico subjects.

In closing, one should note that the expected hypo- and hyperglycemic violations based on the Bergman/gut dynamic model need not coincide with the results of the T1DMS in view of the different levels of complexity of the models. However, it should be noted that the trends are consistent across the models and by increasing the sophistication of the model used to design the controller, one should expect a closer reproduction of results from the T1DMS simulator.

IX. Conclusion

The paper uses a chance constraint framework to pose a robust optimal control problem in the form of a sequential cone programming problem; the solution to which yields a desired open loop robust control profile. In this article, the model of choice has been the Bergman Minimal Model and the resulting controller has been tested on the FDA approved T1DMS simulator. Parametric studies on the impact of the risk tolerance levels for hypo- and hyperglycemic constraints are also carried out and the results are consistent across the simulators. However, the methodology is not limited to this model. Other sophisticated models can also be used to implement the algorithm for better performance.

In addition, this paper discussed the development of control algorithms for an intravenous input. Since most insulin pumps are dedicated to subcutaneous insulin delivery, the algorithm shown would be practical only in a monitored ICU (Intensive Care Unit) environment of a hospital. However, once again the methodology of the algorithm is not limited and can be easily adapted to subcutaneous delivery if an appropriate model for insulin movement from interstices to the bloodstream is augmented.

Moreover, selecting an appropriate target trajectory is also imperative since the algorithm is sensitive to it. This is because different groups of people or patients require different target trajectories (for example: women with gestational diabetes have hyperglycemia thresholds of 140 mg/dL) which are more feasible and relevant to their specific conditions.

References

[1] B. W. Bequette, "Challenges and recent progress in the development of a closed-loop artificial pancreas," *Ann. Rev. Control*, vol. 36, no. 2, pp. 255–266, 2012.

[2] L. Magni, D. M. Raimondo, C. Dalla Man, G. De Nicolao, B. Kovatchev, and C. Cobelli, "Model predictive control of glucose concentration in Type I diabetic patients: An in silico trial," *Biomed. Signal Process. Control*, vol. 4, no. 4, pp. 338–346, 2009.

[3] Y. Ramprasad, G. Rangaiah, and S. Lakshminarayanan, "Enhanced IMC for glucose control in Type 1 diabetics using a detailed physiological model," *Food Bioproducts Process.*, vol. 84, no. 3, pp. 227–236, 2006.

[4] A. Abu-Rmileh, W. Garcia-Gabin, and D. Zambrano, "Internal model sliding mode control approach for glucose regulation in Type 1 diabetes," *Biomed. Signal Process. Control*, vol. 5, no. 2, pp. 94–102, 2010.

[5] K. Lunze, T. Singh, M. Walter, M. D. Brendel, and S. Leonhardt, "Blood glucose control algorithms for Type 1 diabetic patients: A methodological review," *Biomed. Signal Process. Control*, vol. 8, no. 2, pp. 107–119, 2013.

[6] J. Lin *et al.*, "Stochastic modelling of insulin sensitivity and adaptive glycemic control for critical care," *Comput. Methods Programs Biomed.*, vol. 89, no. 2, pp. 141–152, 2008.

[7] S. Nandi, T. Singh, L. D. Mastrandrea, and P. Singla, "Optimal meal time after bolusing for Type 1 diabetes patients under meal uncertainties," in *Proc. IEEE Amer. Control Conf.*, 2017, pp. 4412–4417.

[8] R. S. Parker, F. J. Doyle, J. H. Ward, and N. A. Peppas, "Robust H glucose control in diabetes using a physiological model," *AIChE J.*, vol. 46, no. 12, pp. 2537–2549, 2000.

[9] A. K. Duun-Henriksen *et al.*, "Model identification using stochastic differential equation grey-box models in diabetes," *J. Diabetes Sci. Technol.*, vol. 7, no. 2, pp. 431–440, 2013.

[10] R. N. Bergman, L. S. Phillips, and C. Cobelli, "Physiologic evaluation of factors controlling glucose tolerance in man: Measurement of insulin sensitivity and beta-cell glucose sensitivity from the response to intravenous glucose," *J. Clinical Investigation*, vol. 68, no. 6, pp. 1456–1467, 1981.

[11] C. D. Man, F. Micheletto, D. Lv, M. Breton, B. Kovatchev, and C. Cobelli, "The UVA/padova Type 1 diabetes simulator: New features," *J. Diabetes Sci. Technol.*, vol. 8, no. 1, pp. 26–34, 2014.

[12] N. Adurthi, P. Singla, and T. Singh, "Conjugate unscented transformation: Applications to estimation and control," *J. Dyn. Syst., Meas., Control*, vol. 140, no. 3, 2018, Art. no. 030907.

[13] C. Dalla Man, M. Camilleri, and C. Cobelli, "A system model of oral glucose absorption: validation on gold standard data," *IEEE Trans. Biomed. Eng.*, vol. 53, no. 12, pp. 2472–2478, Dec. 2006.

[14] G. Pacini and R. N. Bergman, "Minmod: A computer program to calculate insulin sensitivity and pancreatic responsivity from the frequently sampled intravenous glucose tolerance test," *Comput. Methods Programs Biomed.*, vol. 23, no. 2, pp. 113–122, 1986.

[15] C. Dalla Man, R. A. Rizza, and C. Cobelli, "Meal simulation model of the glucose-insulin system," *IEEE Trans. Biomed. Eng.*, vol. 54, no. 10, pp. 1740–1749, Oct. 2007.

[16] S. M. Lynch and B. W. Bequette, "Model predictive control of blood glucose in Type I diabetics using subcutaneous glucose measurements," in *Proc. Amer. Control Conf.*, 2002, pp. 4039–4043.

[17] U. D. o. H. US Department of Agriculture and H. Services, "Dietary guidelines for americans, 2010," 2010.

[18] A. D. Association, *Carbohydrate Counting*. Accessed: Aug. 17, 2017. [Online]. http://www.diabetes.org/food-and-fitness/food/what-can-i-eat/understanding-carbohydrates/carbohydrate-counting.html

[19] R. Madankan, P. Singla, T. Singh, and P. D. Scott, "Polynomial-chaos-based Bayesian approach for state and parameter estimations," *J. Guid., Control, Dyn.*, vol. 36, no. 4, pp. 1058–1074, 2013.

[20] S. J. Julier and J. K. Uhlmann, "New extension of the Kalman filter to nonlinear systems," in *Proc. SPIE 3068, Signal Process., Sensor Fusion, and Target Recogn. VI,* 1997, pp. 182–193.

[21] E. R. Seaquist *et al.*, "Hypoglycemia and diabetes: A report of a workgroup of the american diabetes association and the endocrine society," *Diabetes Care*, vol. 36, no. 5, pp. 1384–1395, 2013. [Online]. Available: http://care.diabetesjournals.org/content/36/5/1384

[22] A. D. Association, *Checking Your Blood Glucose.* Accessed: Aug. 18, 2016. [Online]. Available: http://www.diabetes.org/living-with-diabetes/treatment-and-care/blood-glucose-control/checking-your-blood-glucose.html

[23] G. C. Calafiore and L. El Ghaoui, "On distributionally robust chance-constrained linear programs," *J. Optim. Theory Appl.*, vol. 130, no. 1, pp. 1–22, 2006.

[24] I. CVX Research, "CVX: MATLAB software for disciplined convex programming, version 2.0," Aug. 2017. [Online]. Available: http://cvxr.com/cvx

[25] A. D. Association, "How do insulin pumps work?" 2015. [Online]. Available: http://www.diabetes.org/living-with-diabetes/treatment-and-care/medication/insulin/how-do-insulin-pumps-work.html

[26] S. Chen, J. Weimer, M. R. Rickels, A. Peleckis, and I. Lee, "Towards a model-based meal detector for Type i diabetics," *in Proc. 6th Workshop Med. Cyber-Phys. Syst.*, 2015.

[27] S. Zavitsanou, A. Mantalaris, M. C. Georgiadis, and E. N. Pistikopoulos, "In silico closed-loop control validation studies for optimal insulin delivery in Type 1 diabetes," *IEEE Trans. Biomed. Eng.*, vol. 62, no. 10, pp. 2369–2378, Oct. 2015.

[28] I. H. S. Group *et al.*, "Glucose concentrations of less than 3.0 mmol/l (54 mg/dl) should be reported in clinical trials: A joint position statement of the american diabetes association and the european association for the study of diabetes," *Diabetes Care*, vol. 40, no. 1, pp. 155–157, 2017.

[29] A. Bemporad and M. Morari, "Robust model predictive control: A survey," *Robustness Identification Control*, vol. 245, pp. 207–226, 1999.

[30] D. Rodbard, "Metrics to evaluate quality of glycemic control: Comparison of time in target, hypoglycemic, and hyperglycemic ranges with risk indices," *Diabetes Technol. Therapeutics*, vol. 20, no. 5, pp. 325–334, 2018.